Atmospheric Environment 229 (2020) 117476

Contents lists available at ScienceDirect

Atmospheric Environment

journal homepage: http://www.elsevier.com/locate/atmosenv

Short communication

# Effects of cool roofs on turbulent coherent structures and ozone air quality in Seoul

Beom-Soon Han [a], Jong-Jin Baik [a,*], Kyung-Hwan Kwak [b], Seung-Bu Park [c]

[a] School of Earth and Environmental Sciences, Seoul National University, Seoul, South Korea
[b] School of Natural Resources and Environmental Science, Kangwon National University, Chuncheon, South Korea
[c] Korea Institute of Atmospheric Prediction Systems, Seoul, South Korea

## HIGHLIGHTS

- Effects of cool roofs on turbulent flows and ozone air quality in Seoul are examined.
- Cool roofs weaken sea breeze and turbulent coherent structures.
- Advection of $O_3$ into Seoul by sea breeze is weakened.
- Upward transport of $O_3$ precursors by turbulent coherent structures is weakened.
- Cool roofs modify the spatial distribution of $O_3$ concentration.

## ARTICLE INFO

*Keywords:*
Cool roofs
Turbulent coherent structure
Air quality
WRF-CMAQ model
Seoul

## ABSTRACT

The cool-roof strategy is an effective way of mitigating severe urban heat islands, and its impacts on urban flow and air quality deserve in-depth investigations. This study examines the effects of cool roofs on turbulent coherent structures and ozone air quality in Seoul, South Korea using the Weather Research and Forecasting-Community Multiscale Air Quality (WRF-CMAQ) model with a 50 m horizontal grid spacing. Cool roofs decrease the daily average air temperature, planetary boundary layer (PBL) height, and wind speed in the urban area of Seoul by 0.80 °C, 230 m, and 0.17 m $s^{-1}$, respectively. Due to the lowered air temperature by cool roofs, the sea breeze and convective structures weaken and eddies at the PBL top appear less frequently. Since high $O_3$ concentration air flows into Seoul by the sea breeze, the weakened sea breeze decreases the daily average $O_3$ concentration near the surface by 3.3 ppb. Air at lower level is transported upward across the PBL top by convective structures and eddies at the PBL top. The transported air at lower level has lower $O_3$ concentration and higher concentrations of $O_3$ precursors than air at upper level. Therefore, the weakened convective structures and less-frequent appearance of eddies at the PBL top by cool roofs weaken the upward transport of $O_3$ precursors at lower level across the PBL top. As a result, the chemical production of $O_3$ and $O_3$ concentration slightly above the PBL top are decreased. An integrated process rate analysis shows that cool roofs weaken the effects of turbulent coherent structures on $O_3$ concentration.

## 1. Introduction

In urban areas, air temperature increases due to land surface characteristics (e.g., imperviousness and low albedo) and heat emitted from anthropogenic sources (e.g., traffics and air-conditioning systems) (Oke, 1982, 1995; Grimmond, 2007; Rizwan et al., 2008). This phenomenon, known as the urban heat island (UHI), has adverse effects on humans, such as $O_3$ air quality deterioration (Akbari et al., 2001) and an increase of cooling energy consumption (Li et al., 2019). Many strategies, such as cool roofs, green roofs, and urban parks, are suggested to mitigate UHIs. Among them, the cool-roof strategy, which is a strategy to decrease air temperature by increasing roof albedo, is often used in urban areas because it is easy to apply. Many studies have investigated the cooling effects of cool roofs (Oleson et al., 2010; Akbari et al., 2012; Li et al., 2014). By reviewing previous studies, Santamouris (2014) found that the air temperature in urban areas decreases by 0.2 °C as cool roofs increase roof albedo by 0.1.

Cool roofs also influence the flow and planetary boundary layer

* Corresponding author. School of Earth and Environmental Sciences, Seoul National University, Seoul, 08826, South Korea.
*E-mail address:* jjbaik@snu.ac.kr (J.-J. Baik).

https://doi.org/10.1016/j.atmosenv.2020.117476
Received 20 November 2019; Received in revised form 25 February 2020; Accepted 4 April 2020
Available online 7 April 2020

(PBL) in urban areas (Li et al., 2014; Georgescu, 2015; Sharma et al., 2016; Chen and Zhang, 2018; Song et al., 2018). In urban areas, cool roofs decrease the near-surface air temperature, PBL height, and turbulent kinetic energy in the PBL. Vertical motions in the PBL are also weakened, reducing vertical mixing between high-speed air at upper level and low-speed air at lower level. As a result, vertical momentum exchange between upper level and lower level is weakened; thus the wind speed increases at upper level and decreases at lower level (Sharma et al., 2016). Additionally, cool roofs decrease the maximum convective available potential energy in an urban core area, decreasing convective precipitation (Song et al., 2018). Regional-scale flows in urban areas can also be affected by cool roofs. For example, Chen and Zhang (2018) showed that cool roofs decrease the near-surface air temperature in an urban area and reduce the air temperature difference between the urban area and nearby lake, causing weakened lake breezes. As a result, exchanges of heat and moisture between the urban area and nearby lake by the lake breezes are also weakened.

There have been some studies investigating the effects of cool roofs on air quality in urban areas (Taha, 1997, 2008; Fallmann et al., 2016; Touchaei et al., 2016; Epstein et al., 2017). In urban areas, decreased PBL height, weakened vertical motions in PBL, and lowered wind speed induced by cool roofs can cause air stagnation. As a result, concentrations of primary pollutants (e.g., $NO_x$) are generally increased (Fallmann et al., 2016; Epstein et al., 2017; Falasca and Curci, 2018). Concentration changes in secondary pollutants (e.g., $O_3$) due to cool roofs are more complex because cool roofs not only induce air stagnation but also change chemical reactions of secondary pollutants. For example, Taha (1997, 2008, 2015) found that cool roofs decrease $O_3$ concentration in an urban area because the lowered air temperature due to cool roofs reduces chemical production of $O_3$. Also, the modified regional-scale flows due to cool roofs can affect inflow of chemical precursors into urban areas, changing chemical production of secondary pollutants.

Previous cool-roof studies show that cool roofs modify regional-scale flows and air quality in urban areas. Smaller-scale turbulent coherent structures (e.g., convective structures) and associated pollutant concentrations in urban areas can be considerably affected by cool roofs. However, no attempt is made to investigate the effects of cool roofs on turbulent coherent structures and associated air quality. In this study, we extend the study of Han et al. (2019) by considering cool roofs to examine the change of turbulent coherent structures due to cool roofs and its effects on $O_3$ air quality in Seoul, South Korea.

## 2. Methodology

In this study, the Community Multiscale Air Quality (CMAQ) model version 5.2 (Byun and Schere, 2006) coupled with the Weather Research and Forecasting (WRF) model version 3.8.1 (Skamarock et al., 2008) is used. The simulation settings of the WRF-CMAQ model are the same as those in Han et al. (2019), except that an additional simulation considering cool roofs is performed. In the WRF model simulation, five computational domains are considered with horizontal grid spacings of 31.25 km, 6.25 km, 1.25 km, 0.25 km, and 50 m. The Yonsei University (YSU) PBL scheme (Hong et al., 2006) is used for the three outermost domains. For the two innermost domains, the large-eddy simulation (LES) mode in the WRF model is used. In the LES mode of the WRF model, eddy diffusivities for momentum and heat are calculated using the 1.5-order turbulent kinetic energy closure (Deardorff, 1980; Moeng, 1984). In the CMAQ model simulation, three computational domains are considered with horizontal grid spacings of 1.25 km, 0.25 km, and 50 m. Fig. 1 shows land-use/land-cover types in the second innermost domain covering Seoul and the surrounding areas. The three computational domains in the CMAQ model simulation are almost the same as the three innermost domains in the WRF model simulation. In this study, simulation data of the innermost domain covering a central urban area of Seoul are analyzed. The data obtained from the WRF model simulation are used as meteorology input data for the CMAQ model simulation. For

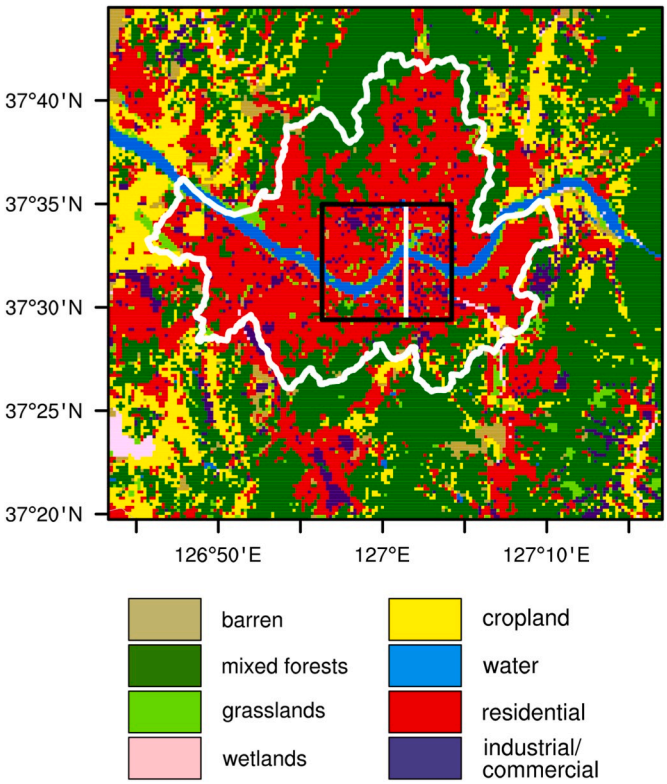


**Fig. 1.** Land-use/land-cover types in the second innermost domain in the CMAQ model simulation. The boundary of Seoul is indicated by the thick white line, and the innermost domain is indicated by the black rectangle. Vertical cross-sections for Fig. 4 are drawn along the white line. (For interpretation of the references to colour in this figure legend, the reader is referred to the Web version of this article).

the eddy diffusivity for reactive pollutants in the two innermost domains in the CMAQ model simulation, the eddy diffusivity for heat calculated from the WRF-LES model is used. The WRF-CMAQ model is integrated for 39 h from 0900 LT (= UTC + 9 h) 4 to 2400 LT 5 June 2010, and the simulation data of 5 June 2010 are analyzed. Detailed descriptions of the simulation settings are given in Han et al. (2019).

A simulation with cool roofs (COOL case) is performed, and its results are compared to those of the simulation with conventional roofs (CONV case). The CONV case is identical to the simulation in Han et al. (2019). In the CONV case, the roof albedo in urban areas is 0.2. In the COOL case, the roof albedo is increased from 0.2 to 0.85 to represent cool roofs. This increase of the roof albedo is applied to urban areas (represented by residential and industrial/commercial land-use/land-cover, see Fig. 1). The urban fractions in the residential and industrial/commercial LULC are 0.9 and 0.95, respectively. The WRF-CMAQ model is validated by comparing the simulation results of the CONV case and the observed data (Han et al., 2019). The model reproduces the diurnal variations of the near-surface air temperature, wind speed, and $O_3$ concentration in Seoul well (see Figs. 2 and 3 in Han et al. (2019)).

## 3. Results and discussion

The diurnal variations of 2-m air temperature, PBL height, 10-m wind speed, squared vertical wind speed at the second lowest model level ($z \sim 100$ m, $z$: height above the sea level), sensible heat flux, and latent heat flux averaged over the urban LULC in the CONV and COOL cases are compared (Fig. 2). Due to the increased albedo of cool roofs, the averaged 2-m air temperature and PBL height in the COOL case are lower than those in the CONV case, especially in the daytime (Fig. 2a and b). In the early morning and nighttime, the differences in the

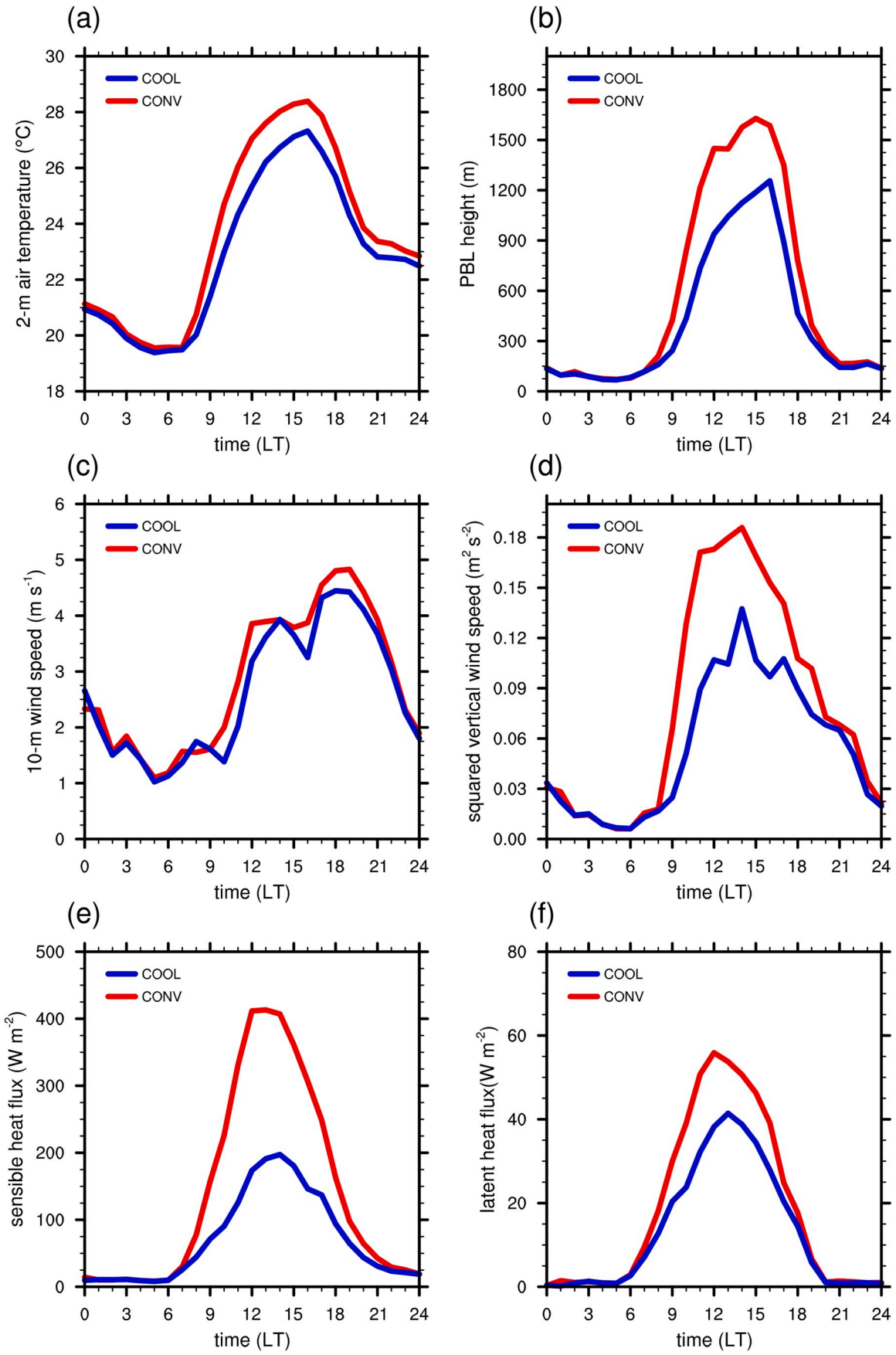


**Fig. 2.** Diurnal variations of (a) 2-m air temperature, (b) PBL height, (c) 10-m wind speed, (d) squared vertical wind speed at the second lowest model level, (e) sensible heat flux, and (f) latent heat flux averaged over the urban LULC in the CONV and COOL cases.

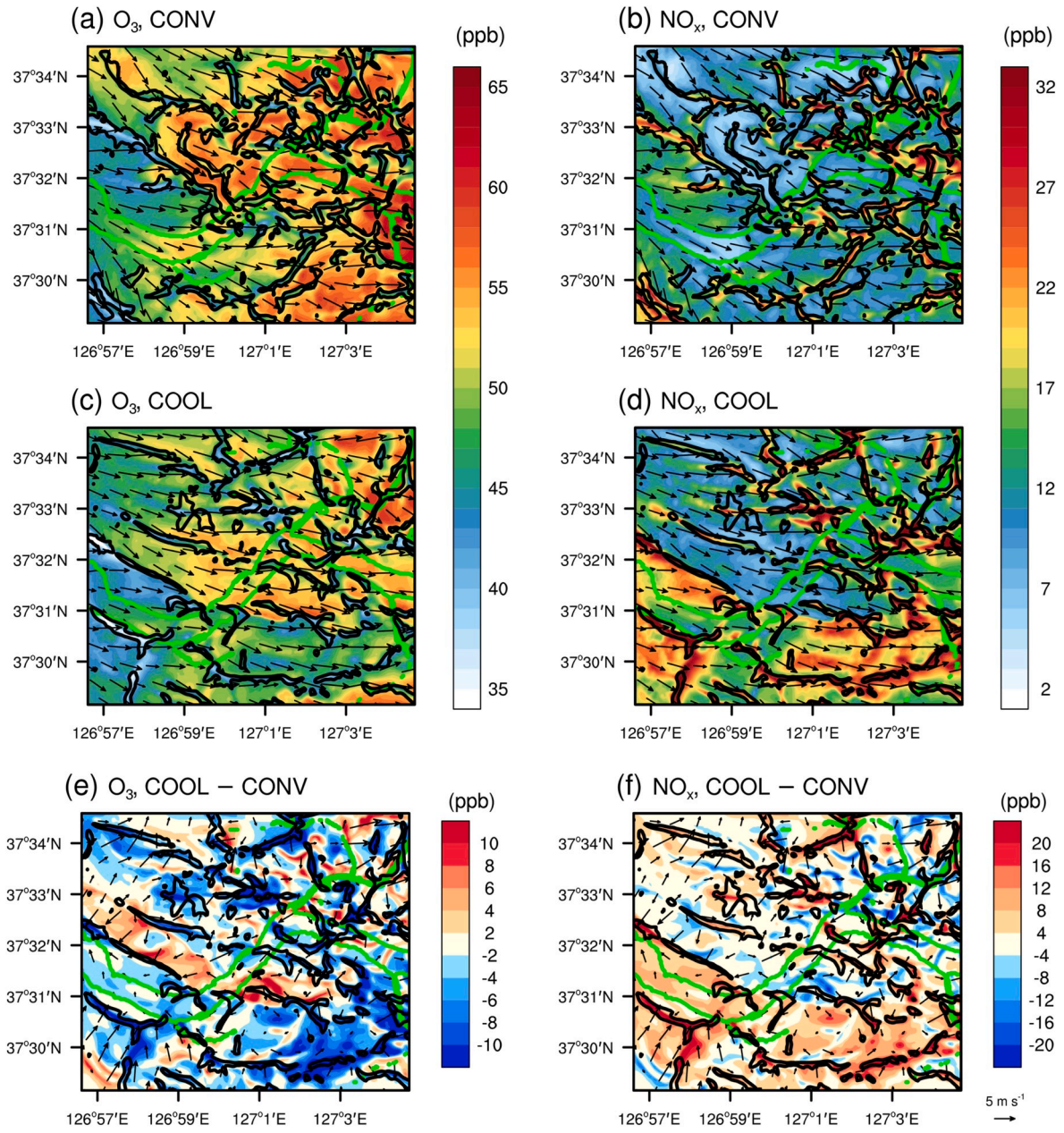


**Fig. 3.** (a) $O_3$ and (b) $NO_x$ concentrations and horizontal wind vector at the second lowest model level at 1400 LT in the CONV case. (c) and (d) are the same as (a) and (b) except for in the COOL case. Differences in (e) $O_3$ and (f) $NO_x$ concentrations and horizontal wind vector between the COOL and CONV cases at 1400 LT. The contours of vertical velocity of 0.5 m $s^{-1}$ at the second lowest model level are added (black contour lines). The Han River and its tributaries are indicated by the green lines. (For interpretation of the references to colour in this figure legend, the reader is referred to the Web version of this article).

averaged 2-m air temperature and PBL height are very small because there is very little or no sunlight to be reflected by cool roofs. The daily average differences in the averaged 2-m air temperature and PBL height between the COOL and CONV cases are −0.80 °C and −230 m, respectively. The maximum 2-m air temperature difference is −1.7 °C at 1200 LT, and the maximum PBL height difference is −510 m at 1200 LT. The lower air temperature in the COOL case weakens the sea breeze and vertical motions related to convective structures in Seoul. As a result, the averaged 10-m wind speed and squared vertical wind speed in the COOL case are decreased (Fig. 2c and d). Cool roofs decrease the daily averages of the averaged 10-m wind speed and squared vertical wind speed by 0.17 m $s^{-1}$ and 0.032 $m^2$ $s^{-2}$, respectively. The increased albedo of cool roofs decreases the surface temperature in urban LULC, resulting in the decreases of the averaged sensible and latent heat fluxes in the daytime (Fig. 2e and f). Compared to the CONV case, the daily averages of the averaged sensible heat flux and latent heat flux in the COOL case are decreased by 84 W $m^{-2}$ and 6 W $m^{-2}$, respectively.

The sea breeze and convective structures modified by cool roofs can affect air quality in Seoul. Fig. 3 shows $O_3$ and $NO_x$ concentrations and horizontal wind vector at 1400 LT at the second lowest model level in the CONV and COOL cases. The differences between the COOL and CONV cases (COOL case – CONV case) are also shown in Fig. 3. At 1400 LT, the westerly to northwesterly sea breeze and convective structures appear in both cases. Updrafts related to convective structures in the COOL case appear in narrower areas compared to those in the CONV case, indicating that cool roofs weaken convective structures. Air in the west to northwest of Seoul is brought into Seoul by the sea breeze. Since the air brought into Seoul generally has higher $O_3$ and lower $NO_x$ concentrations than air in Seoul (Han et al., 2019), the weakened sea breeze by cool roofs generally decreases and increases $O_3$ and $NO_x$

concentrations in Seoul, respectively (e.g., the lower $O_3$ and higher $NO_x$ concentrations in the COOL case at and near (~126° 58′E, ~37° 30′N) in Fig. 3e and f). Updrafts related to convective structures transport air at lower level upward. Since NO, which can decompose $O_3$, is usually emitted near the surface, the transported air at lower level generally has lower $O_3$ and higher $NO_x$ concentrations than air at upper level. Therefore, $O_3$ and $NO_x$ concentrations in updraft areas are lower and higher than those in other areas, respectively (Han et al., 2019). Additionally, cool roofs change the locations of updraft areas; thus the spatial distribution of $O_3$ and $NO_x$ concentrations in the CONV and COOL cases are significantly different.

To compare the effects of convective structures on $O_3$ dispersion in the CONV and COOL cases, vertical cross-sections of $O_3$ concentration and wind vector at 1400 LT in the CONV case and at 1400 LT and 1600 LT in the COOL case are shown in Fig. 4. At 1400 LT, vertical motions related to convective structures in the COOL case are weaker than those in the CONV case because cool roofs weaken convective structures. As a result, the upward transport of $O_3$ by updrafts related to convective structures are weakened in the COOL case. In the CONV case, the sea breeze circulation causes different wind directions above and below the PBL top. Therefore, at the PBL top, the strong vertical wind shear appears and induces clockwise-rotating eddies (e.g., an eddy at ~37° 34′N in Fig. 4a) (Han et al., 2019). In the vertical cross-section of $O_3$ concentration and wind vector at 1400 LT in the COOL case, eddies at the PBL top do not appear because cool roofs weaken the sea breeze circulation and thus the vertical wind shear at the PBL top (Fig. 4b). In the COOL case, eddies at the PBL top appear at times when the vertical shear at the PBL top is enhanced, but the appearance frequency of eddies at the PBL top is significantly lower than that in the CONV case. The eddy at the PBL top in the COOL case seen at such a time is illustrated in Fig. 4c. Airs above and below the PBL top are mixed by eddies at the PBL top, so that air at lower level is transported upward across the PBL top (Han et al., 2019). Since cool roofs decrease the appearance frequency of eddies at the PBL top, the upward transport of $O_3$ precursors at lower level (e.g., $NO_x$ and isoprene) across the PBL top in the COOL case is weaker than that in the CONV case. As a result, slightly above the PBL top, the chemical production of $O_3$ is decreased and $O_3$ concentration in the COOL case is smaller than that in the CONV case (Fig. 4b).

The diurnal variation of $O_3$ concentration at the second lowest model level and vertical profiles of $O_3$ concentration at 0900, 1200, 1500, and 1800 LT averaged over the urban LULC in the CONV and COOL cases are presented in Fig. 5. In the COOL case, the averaged near-surface $O_3$ concentration is lower than that in the CONV case because the weakened sea breeze reduces the advection of $O_3$ into Seoul (Fig. 5a). The daily average difference in the averaged near-surface $O_3$ concentration between the COOL and CONV cases is −3.3 ppb.

At 0900 and 1200 LT, the differences in the averaged $O_3$ concentration between the COOL and CONV cases are relatively small compared to those at 1500 and 1800 LT (Fig. 5b). It seems that the sea breeze and convective structures weakened by cool roofs are less-developed; thus the effects of cool roofs on $O_3$ concentration are weak at 0900 and 1200 LT. At 1500 LT, the averaged $O_3$ concentration above the PBL top ($z \sim$ 1.3–2.5 km) in the COOL case is lower than that in the CONV case. This is because cool roofs reduce the chemical production of $O_3$ above the PBL top by reducing the upward transport of $O_3$ precursors due to turbulent coherent structures. At 1800 LT, the averaged $O_3$ concentration at upper level ($z \sim$ 1.0–2.5 km) in the CONV case is decreased because the chemical production of $O_3$ at upper level is reduced. In contrast, the averaged $O_3$ concentration at upper level in the COOL case is generally increased because high $O_3$ concentration air at upper level is transported into Seoul. As a result, at upper level, the averaged $O_3$ concentration is larger in the COOL case or the magnitude of the difference between the averaged $O_3$ concentrations in the CONV and COOL cases is decreased. The temporal changes of the vertical profiles of the averaged $O_3$ concentration show that the effects of cool roofs on $O_3$ concentration is complex, which requires consideration of

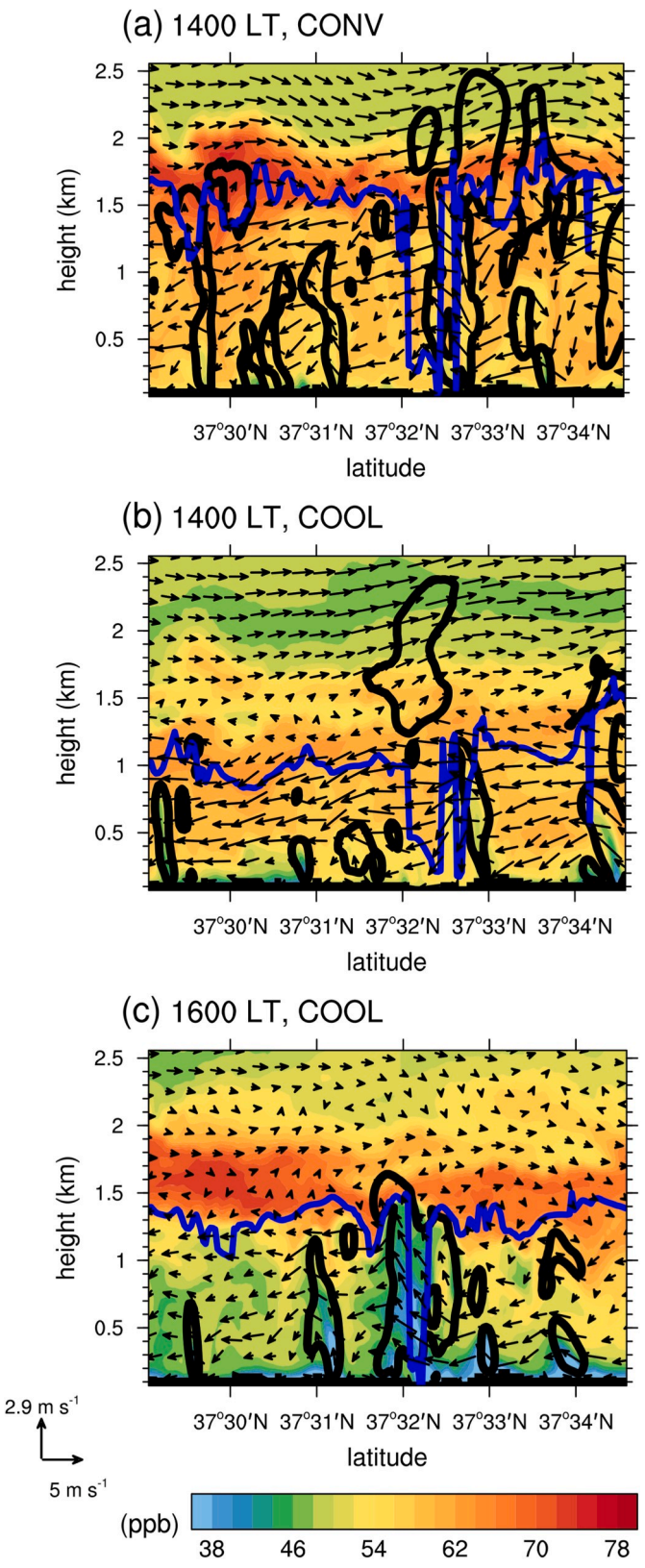


**Fig. 4.** Vertical cross-sections of $O_3$ concentration and wind vector along the black line in Fig. 1 at (a) 1400 LT in the CONV case and at (b) 1400 LT and (c) 1600 LT in the COOL case. The contours of vertical velocity of 0.5 m $s^{-1}$ are added (black contour lines). The PBL height is represented by the blue lines. (For interpretation of the references to colour in this figure legend, the reader is referred to the Web version of this article).

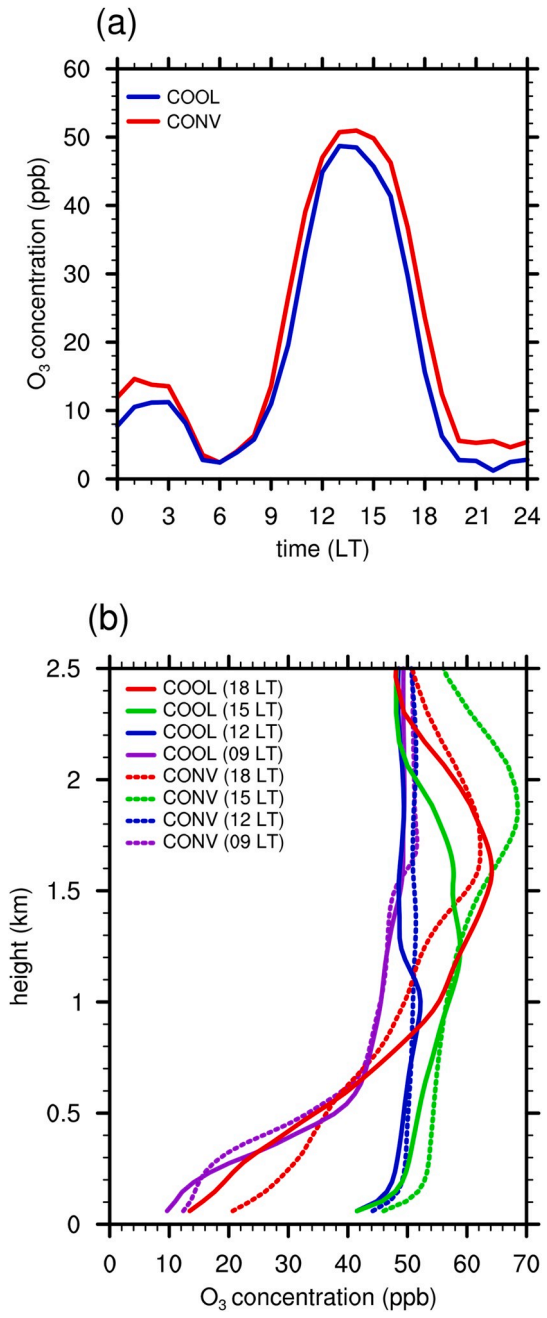


**Fig. 5.** (a) Diurnal variations of $O_3$ concentration at the second lowest model level and (b) vertical profiles of $O_3$ concentrations at 0900, 1200, 1500, and 1800 LT averaged over the urban LULC in the CONV and COOL cases.

both turbulent flows and chemical reactions of pollutants.

To further examine the effects of cool roofs on $O_3$ air quality, an integrated process rate (IPR) analysis (Gipson, 1999) is performed. The IPR analysis shows how each process (e.g., advection process) contributes to $O_3$ concentration (Jeffries and Tonnesen, 1994). The vertical profiles of the contributions of individual processes averaged over the urban LULC and the period from 1445 LT to 1515 LT are presented in Fig. 6. Near the surface (below $z \sim 0.3$ km), the positive contribution of the horizontal advection process in the COOL case is smaller than that in the CONV case because the horizontal advection of $O_3$ into Seoul by the sea breeze is weakened by cool roofs. The magnitude of the negative contribution of the vertical advection process below $z \sim 0.3$ km in the COOL case is smaller than that in the CONV case, indicating that the amount of $O_3$ transported from lower level to upper level by convective

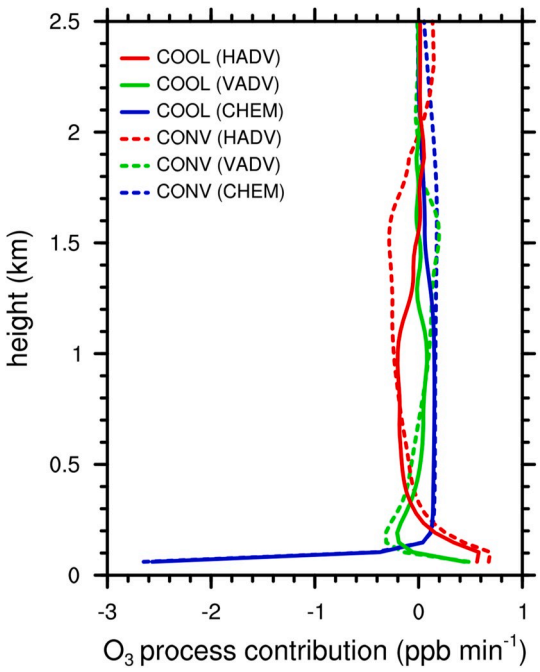


**Fig. 6.** Vertical profiles of the contributions of individual processes [horizontal advection (HADV), vertical advection (VADV), and chemical (CHEM) processes] to $O_3$ concentration averaged over the urban LULC and the period from 1445 to 1515 LT in the CONV and COOL cases.

structures is decreased due to cool roofs. The contributions of the chemical process in the CONV and COOL cases are similar. These results support that $O_3$ concentration near the surface in the COOL case is decreased mainly due to the weaker horizontal advection of $O_3$ into Seoul. Between $z \sim 1$ km and $z \sim 2$ km, the magnitude of the contribution of the horizontal advection process is smaller in the COOL case. It seems that the horizontally divergent flow of low $O_3$ concentration air transported from lower level is weakened due to cool roofs. Above $z \sim 1$ km, the chemical process in the COOL case is smaller than that in the CONV case because cool roofs decrease the chemical production of $O_3$ at upper level. Fig. 6 shows the effects of the aforementioned phenomena induced by cool roofs (e.g., the weakened convective structures and the decreased appearance frequency of eddies at the PBL top) on $O_3$ concentration.

The enhanced solar radiation reflection by cool roofs increases actinic flux and thus can affect the photochemistry of pollutants. To get some insight into the increased actinic flux due to cool roofs and its effects on the photochemistry of pollutants, an additional simulation (AFX case) is performed. In the AFX case, the increased actinic flux due to cool roofs is calculated using the radiation output data from the WRF model and applied to the photochemistry in the CMAQ model. Fig. 7 shows the diurnal variations of actinic flux, photolysis rate of $NO_2$ ($J_{NO_2}$), and $O_3$ concentration at the lowest model level averaged over the urban LULC in the AFX and COOL cases. The increased albedo of cool roofs increases the averaged actinic flux in the daytime (Fig. 7a), and the daily average of the averaged actinic flux increases by 130 W $m^{-2}$. As a result, the averaged $J_{NO_2}$ and $O_3$ concentration are also increased (Fig. 7b and c). The increased actinic flux by cool roofs increases the daily averages of the averaged $J_{NO_2}$ and $O_3$ concentration by 0.11 $min^{-1}$ and 3.3 ppb, respectively. The magnitude of this daily averaged $O_3$ concentration increase is about the same as that of the daily averaged $O_3$ concentration decrease in the COOL case compared to the CONV case (3.3 ppb). This result implies that the effects of increased actinic flux and modified meteorology on $O_3$ concentration can considerably cancel each other. Further in-depth studies are needed to evaluate these two effects of cool roofs on air quality in detail.

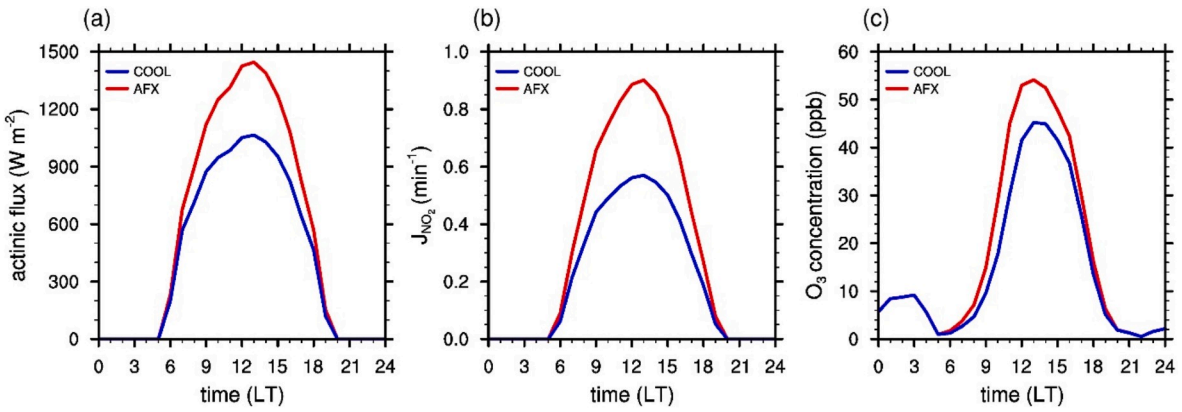


**Fig. 7.** Diurnal variations of (a) actinic flux, (b) photolysis rate of $NO_2$ ($J_{NO_2}$), and (c) $O_3$ concentration at the lowest model level averaged over the urban LULC in the AFX and COOL cases.

## 4. Summary and conclusions

The effects of cool roofs on turbulent coherent structures and $O_3$ air quality in Seoul were investigated using the WRF-CMAQ model with a 50 m horizontal grid spacing. Due to the increased roof albedo of cool roofs, the air temperature, PBL height, wind speed, sensible heat flux, and latent heat flux in Seoul are decreased, especially in the daytime. Additionally, cool roofs weaken the sea breeze, which brings high $O_3$ concentration air into Seoul, and thus $O_3$ concentration in Seoul is decreased. $O_3$ precursors (e.g., $NO_x$) at lower level is transported across the PBL top by updrafts related to convective structures and eddies at the PBL top. Since cool roofs weaken convective structures and decrease the appearance frequency of eddies at the PBL top, the upward transport of $O_3$ precursors at lower level is reduced. In the middle of the day, the reduced upward transport of $O_3$ precursors decreases the chemical production of $O_3$ slightly above the PBL top. To further examine the effects of cool roofs on $O_3$ air quality, the process analysis was performed. The process analysis shows that the weakened sea breeze due to cool roofs is the main reason for the decreased $O_3$ concentration near the surface. Also, the process analysis shows that cool roofs weaken the effects of turbulent coherent structures on $O_3$ concentration in and slightly above the PBL.

This study investigates the effects of cool roofs on turbulent coherent structures and $O_3$ air quality in summer. In different seasons, the amount of sunlight is decreased; thus the effects of cool roofs can vary. Further studies that investigate the relationship between the amount of sunlight and the effects of cool roofs are required.

## Declaration of competing interest

The authors declare that they have no known competing financial interests or personal relationships that could have appeared to influence the work reported in this paper.

## CRediT authorship contribution statement

**Beom-Soon Han:** Conceptualization, Methodology, Software, Visualization, Formal analysis, Investigation, Writing - original draft, Writing - review & editing. **Jong-Jin Baik:** Conceptualization, Methodology, Formal analysis, Investigation, Writing - review & editing, Supervision, Resources, Project administration, Funding acquisition. **Kyung-Hwan Kwak:** Methodology, Formal analysis, Investigation, Writing - review & editing. **Seung-Bu Park:** Methodology, Formal analysis, Investigation, Writing - review & editing.

## Acknowledgements

The authors are grateful to two anonymous reviewers for providing valuable comments on this work. This work was supported by Basic Science Research Program through the National Research Foundation of Korea (NRF) funded by the Ministry of Science and ICT (No. 2016R1A2B2013549).

## References

Akbari, H., Pomerantz, M., Taha, H., 2001. Cool surfaces and shade trees to reduce energy use and improve air quality in urban area. Sol. Energy 70, 295–310.
Akbari, H., Matthews, H.D., Seto, D., 2012. The long-term effect of increasing the albedo of urban areas. Environ. Res. Lett. 7, 024004 https://doi.org/10.1088/1748-9326/7/2/024004.
Byun, D., Schere, K.L., 2006. Review of the governing equations, computational algorithms, and other components of the models-3 community multiscale air quality (CMAQ) modeling system. Appl. Mech. Rev. 59, 51–77.
Chen, Y., Zhang, N., 2018. Urban heat island mitigation effectiveness under extreme heat conditions in the Suzhou–Wuxi–Changzhou metropolitan area, China. J. Appl. Meteorol. Clim. 57, 235–253.
Deardorff, J.W., 1980. Stratocumulus-capped mixed layers derived from a three-dimensional model. Boundary-Layer Meteorol. 18, 495–527.
Epstein, S.A., Lee, S.-M., Katzenstein, A.S., Carreras-Sospedra, M., Zhang, X., Farina, S.C., Vahmani, P., Fine, P.M., Ban-Weiss, G., 2017. Air-quality implications of widespread adoption of cool roofs on ozone and particulate matter in southern California. P. Natl. Acad. Sci. 114, 8991–8996.
Falasca, S., Curci, G., 2018. Impact of highly reflective materials on meteorology, PM10 and ozone in urban areas: a modeling study with WRF-CHIMERE at high resolution over Milan (Italy). Urban Sci. 2 https://doi.org/10.3390/urbansci2010018.
Fallmann, J., Forkel, R., Emeis, S., 2016. Secondary effects of urban heat island mitigation measures on air quality. Atmos. Environ. 125, 199–211.
Georgescu, M., 2015. Challenges associated with adaptation to future urban expansion. J. Clim. 28, 2544–2563.
Gipson, G.L., 1999. Science Algorithms of the EPA Models-3 Community Multiscale Air Quality (CMAQ) Modeling System: Process Analysis. EPA/600/R-99/030. US EPA. Online available at: https://www.cmascenter.org/cmaq/science_documentation/pdf/ch16.pdf.
Grimmond, S., 2007. Urbanization and global environmental change: local effects of urban warming. Geogr. J. 173, 83–88.
Han, B.-S., Baik, J.-J., Kwak, K.-H., 2019. A preliminary study of turbulent coherent structures and ozone air quality in Seoul using the WRF-CMAQ model at a 50 m grid spacing. Atmos. Environ. 218, 117012.
Hong, S.-Y., Noh, Y., Dudhia, J., 2006. A new vertical diffusion package with an explicit treatment of entrainment processes. Mon. Weather Rev. 134, 2318–2341.
Jeffries, H.E., Tonnesen, S., 1994. A comparison of two photochemical reaction mechanisms using mass balance and process analysis. Atmos. Environ. 28, 2991–3003.
Li, D., Bou-Zeid, E., Oppenheimer, M., 2014. The effectiveness of cool and green roofs as urban heat island mitigation strategies. Environ. Res. Lett. 9, 055002 https://doi.org/10.1088/1748-9326/9/5/055002.
Li, X., Zhou, Y., Yu, S., Jia, G., Li, H., Li, W., 2019. Urban heat island impacts on building energy consumption: a review of approaches and findings. Energy 174, 407–419.
Moeng, C.-H., 1984. A large-eddy-simulation model for the study of planetary boundary-layer turbulence. J. Atmos. Sci. 41, 2052–2062.
Oke, T.R., 1982. The energetic basis of the urban heat-island. Q. J. R. Meteorol. Soc. 108, 1–24.

Oke, T.R., 1995. The heat island of the urban boundary layer: characteristics, causes and effects. In: Cermak, J.E., Davenport, A.G., Plate, E.J., Viegas, D.X. (Eds.), Wind Climate in Cities. Kluwer Academic Publishers, Dordrecht, pp. 81–107.

Oleson, K.W., Bonan, G.B., Feddema, J., 2010. Effects of white roofs on urban temperature in a global climate model. Geophys. Res. Lett. 37, L03701 https://doi.org/10.1029/2009GL042194.

Rizwan, A.M., Dennis, L.Y.C., Liu, C., 2008. A review on the generation, determination and mitigation of urban heat island. J. Environ. Sci. 20, 120–128.

Santamouris, M., 2014. Cooling the cities – a review of reflective and green roof mitigation technologies to fight heat island and improve comfort in urban environments. Sol. Energy 103, 682–703.

Sharma, A., Conry, P., Fernando, H.J.S., Hamlet, A.F., Hellmann, J.J., Chen, F., 2016. Green and cool roofs to mitigate urban heat island effects in the Chicago metropolitan area: evaluation with a regional climate model. Environ. Res. Lett. 11, 064004 https://doi.org/10.1088/1748-9326/11/6/064004.

Skamarock, W.C., Klemp, J.B., Dudhia, J., Gill, D.O., Barker, D.M., Duda, M.G., Huang, X.-Y., Wang, W., Powers, J.G., 2008. A Description of Advanced Research WRF Version 3. NCAR Technical Note NCAR/TN–475+STR.

Song, J., Wang, Z.-H., Wang, C., 2018. The regional impact of urban heat mitigation strategies on planetary boundary layer dynamics over a semiarid city. J. Geophys. Res. Atmos. 123, 6410–6422.

Taha, H., 1997. Modeling the impacts of large-scale albedo changes on ozone air quality in the South Coast Air Basin. Atmos. Environ. 31, 1667–1676.

Taha, H., 2008. Urban surface modification as a potential ozone air-quality improvement strategy in California: a mesoscale modelling study. Boundary-Layer Meteorol. 127, 219–239.

Taha, H., 2015. Meteorological, air-quality, and emission-equivalence impacts of urban heat island control in California. Sustain. Cities Soc. 19, 207–221.

Touchaei, A.G., Akbari, H., Tessum, C.W., 2016. Effect of increasing urban albedo on meteorology and air quality of Montreal (Canada) – episodic simulation of heat wave in 2005. Atmos. Environ. 132, 188–206.